Inorganic Chemistry
Article

Inorg. Chem. **2009**, *48*, 10211–10221 **10211**
DOI: 10.1021/ic901201s

Molybdenum(VI) Dioxo Complexes with Tridentate Phenolate Ligands

Martina E. Judmaier,[†] Andreas Wallner,[†] Gregor N. Stipicic,[‡] Karl Kirchner,[‡] Judith Baumgartner,[§] Ferdinand Belaj,[†] and Nadia C. Mösch-Zanetti*[,†]

[†]*Institut für Chemie, Bereich Anorganische Chemie, Karl-Franzens-Universität Graz, Schubertstrasse 1, 8010 Graz, Austria,* [‡]*Institut für angewandte Synthesechemie, Technische Universität Wien, Getreidemarkt 9, 1060 Wien, Austria, and* [§]*Institut für Anorganische Chemie, Technische Universität Graz, Stremayrgasse 16, 8010 Graz, Austria*

Received June 23, 2009

A series of new molybdenum(VI) dioxo complexes of the type $[MoO_2ClL^X]$ with potentially monoanionic phenolate ligands L^X (L = 4,6-di-*tert*-butyl-2-{[(X)methylamino]methyl}-phenolate; L^{OMe}, where X = 2′-methoxyethyl; L^{SEt}, where X = 2′-ethylthioethyl; L^{NEt2}, where X = 2′-diethylaminoethyl; and L^{NMe2}, where X = 2′-dimethylaminoethyl) have been synthesized as models for molybdoenzymes. All molybdenum complexes were readily accessible by employing the η^2-coordinate pyrazolate complex $[MoO_2Cl(\eta^2\text{-}t\text{-}Bu_2pz)]$. The nitrogen ligand can easily be exchanged by the monoanionic phenolate ligands L^X in toluene at room temperature, leading to monosubstituted complexes **1**−**4** as yellow to red powders in good yields. Suitable single crystals for X-ray diffraction analysis of complexes **2** and **3** were obtained from a concentrated benzene solution. Both complexes reveal a six-coordinate molybdenum atom in a distorted octahedral surrounding, with a tridentate fac coordination of the ligand. Additionally, the complexes were characterized by elemental analysis; IR, UV/vis, and NMR spectroscopy; and mass spectrometry. For complexes **1** and **2**, only one isomer can be detected in solution, whereas complexes **3** and **4** reveal the formation of two isomers in a 1:1 ratio for **3** and in a 1:3 ratio for **4**. Optimized geometries and relative free energies of all possible isomers have been established by DFT calculations, indicating two isomers in solutions of **3** and **4** to be two types of facially coordinated complexes. Furthermore, this is supported by gauge-independent atomic orbital calculations of the ^{1}H NMR shifts with a high correlation of experimental and calculated shifts for the fac compounds. Oxygen atom transfer reactions of **1** to PMe_3 quickly form monooxo molybdenum compound *cis*,*mer*-$[MoOCl_2(PMe_3)_3]$.

Introduction

Molybdenum is found in a large group of enzymes commonly referred to as *oxotransferases* or *hydroxylases*, depending on whether the substrate is transformed by a primary oxygen atom transfer or a water molecule is involved in the substrate transformation. These enzymes are widespread and catalyze important oxygen atom transfer (OAT) reactions. They can be classified into three different families, *xanthine oxidase*, *sulfite oxidase*, and *DMSO reductase* families, on the basis of the structure of their oxidized active center.[1] The structures of at least one member of most of them have been characterized by X-ray crystallography.[2−4] They all contain a mononuclear molybdenum oxo center that is coordinated by one or two pterin-based ligands. Among the families, the *dimethyl sulfoxide reductase* family is the most diverse, where, in addition to the pterin ligands, the metal is coordinated by a serine alkoxide, a cysteine thiolate, or an aspartate carboxylate. Particular interest was raised regarding *dimethyl sulfoxide reductase* (DMSOR), as it contains molybdopterin as its only cofactor, making it particularly suitable for spectroscopic investigations.[5,6] Despite several crystal structures,[4,7−10] the structure of the active site remains ambiguous and, hence, the reaction mechanism. Thus, there has been some discussion whether the active center is six or seven-coordinate, whether the dithiolene unit of the pterin-based ligand is coordinated in a symmetric or

*To whom the correspondence should be addressed. E-mail: nadia.moesch@uni-graz.at.

(1) Hille, R. *Chem. Rev.* **1996**, 2757–2816.
(2) Romao, M. J.; Archer, M.; Moura, I.; Moura, J. J.; LeGall, J.; Engh, R.; Schneider, M.; Hof, P.; Huber, R. *Science* **1995**, *270*, 1170–1176.
(3) Kisker, C.; Schindelin, H.; Pacheco, A.; Wehbi, W. A.; Garrett, R. M.; Rajagopalan, K. V.; Enemark, J.; Rees, D. C. *Cell* **1997**, *91*, 973–983.
(4) Schindelin, H.; Kisker, C.; Hilton, J.; Rajagopalan, K. V.; Rees, D. C. *Science* **1996**, *272*, 1615–1621.
(5) Bastian, N. R.; Kay, C. J.; Barber, M. J.; Rajagopalan, K. V. *J. Biol. Chem.* **1991**, *266*, 45–51.
(6) Garton, S. D.; Hilton, J.; Oku, H.; Crouse, B. R.; Rajagopalan, K. V.; Johnson, M. K. *J. Am. Chem. Soc.* **1997**, *119*, 12906–12916.
(7) Bray, R. C.; Adams, B.; Smith, A. T.; Bennett, B.; Bailey, S. *Biochemistry* **2000**, *39*, 11258–11269.
(8) Li, H. K.; Temple, C.; Rajagopalan, K. V.; Schindelin, H. *J. Am. Chem. Soc.* **2000**, *122*, 7673–7680.
(9) McAlpine, A. S.; McEwan, A. G.; Shaw, A. L.; Bailey, S. *J. Biol. Inorg. Chem.* **1997**, *2*, 690–701.
(10) Schneider, F.; Löwe, J. H. R.; Schindelin, H.; Kisker, C.; Knäblein, J. *J. Mol. Biol.* **1996**, *263*, 53–69.

Published on Web 09/29/2009

asymmetric fashion, or whether a conformational change such as a cis-to-trans rearrangement of the pterin unit versus the oxo group occurs during the catalytic cycle.[11−13] Although a high-resolution X-ray diffraction analysis of DMSO reductase points to the structural diversities occurring due to different crystallizing or handling conditions of the enzyme, the detailed mechanism remains unclear.[7]

A wide variety of molybdenum compounds have been developed, modeling the active sites of oxotransferases for a better understanding of both structural and functional details.[14,15] Close structural models represent molybdenum dithiolene complexes that have been reported in recent years.[16−22] Oxygen atom transfer functionality has been found in various model compounds.[14,15]

We were intrigued by the above-described structural diversity. For this reason, we prepared molybdenum oxo complexes coordinated by a series of monoanionic phenolate ligands employing various N, O, and S additional donors capable of tridentate coordination. The architecture of the ligands allows for the formation of various coordination isomers. An investigation of OAT reactivity will help in elucidating structural/functional relationships. A literature search revealed that only one molybdenum dioxo system allowed the isolation of coordination isomers with tripodal bis(pyrazolyl)phenolate ligands.[23,24] OAT reactions of both isomers with tertiary phosphines confirm the effect of geometry on the rate of oxygen transfer.[25] However, this system is limited to pyrazol-based additional donors.

During the past few years, phenolate-based ligands have enjoyed much success in the stabilization of metal compounds, which are used in various chemical transformations.[26−29] These ligand types range from simple mono-phenoxide systems through to bis-phenoxide systems, many of which are

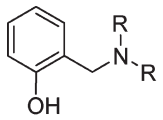

R = alkyl 18

Figure 1. Unsaturated amino phenol fragment of the ligand.

easily obtained via Schiff-base or Mannich condensation reactions.[30−33] The steric and electronic properties of these ligands can be easily turned by variation of the aromatic part or the alkyl chain donor. In 2003, Tolman and co-workers used the chelating tridentate ligand L^{NMe2} for the preparation of highly active zinc catalysts, which catalyzes the lactide polymerization in good control and high yield.[30] Binda et al. used this ligand for the stabilization of lanthanide metals during ring-opening polymerization reactions of cylic esters.[34,35] In 2008, Chen and co-workers used the ligand L^{OMe} for the preparation of a lithium complex, which demonstrates catalytic activity toward the ring-opening polymerization of lactides.[31]

Molybdenum(VI) dioxo complexes with phenol-based ligand systems of the principal type shown in Figure 1 including an amine functionality are known in the literature, mainly bis- and trisphenolate[36−39] and only rarely monoanionic phenolate ligands.[40]

Here, we report the syntheses of novel sterically demanding monophenolate ligands containing a variety of additional O, N, and S donors and their coordination behavior toward the $[MoO_2]^{2+}$ core. Depending on the additional donor, different ratios of coordinational isomers were found. The geometries and relative stabilities of these isomers as well as mechanistic aspects of the formation of the various molybdenum complexes are established by means of DFT/B3LYP calculations.

Results and Discussion

Syntheses of the Ligands. The ligand syntheses follow a three-step procedure starting from inexpensive 2,4-bis-*tert*-butylphenol as shown in Scheme 1. It can be converted into 2-chloromethyl-4,6-di-*tert*-butylphenole, as described in the literature, and subsequent treatment with corresponding secondary amines gives ligands HL^{OMe}, HL^{SEt}, HL^{NEt2}, and HL^{NMe2} as viscous oils or as colorless solids in good yields. After a general workup, they were used without further purification. All ligands were characterized by NMR spectroscopy. The protons of the methylene group at the aromatic ring give rise to characteristic singlets in the region between 3.30 and 4.00 ppm

(11) Jones, R. M.; Inscore, F. E.; Hille, R.; Kirk, M. L. *Inorg. Chem.* **1999**, *38*, 4963–4970.
(12) George, G. N.; Mertens, J. A.; Campell, W. H. *J. Am. Chem. Soc.* **1999**, *121*, 9730–9731.
(13) Heffron, K.; Léger, C.; Rothery, R. A.; Weiner, J. H.; Armstrong, F. A. *Biochemistry* **2001**, *40*, 3117–3126.
(14) Enemark, J.; Cooney, J. J. A.; Wang, J. J.; Holm, R. H. *Chem. Rev.* **2004**, *104*, 1175–1200.
(15) Sugimoto, H.; Tsukube, H. *Chem. Soc. Rev.* **2008**, *37*, 2609–2616.
(16) Lim, B. S.; Sung, K. M.; Holm, R. H. *J. Am. Chem. Soc.* **2000**, *122*, 7410–7411.
(17) Lim, B. S.; Holm, R. H. *J. Am. Chem. Soc.* **2001**, *123*, 1920–1930.
(18) Lim, B. S.; Willer, M. W.; Miao, M.; Holm, R. H. *J. Am. Chem. Soc.* **2001**, *123*, 8343–8349.
(19) Sugimoto, H.; Suyama, K.; Sugimoto, K.; Miyake, H.; Takahashi, I.; Hirota, S.; Itoh, S. *Inorg. Chem.* **2008**, *47*, 10150–10157.
(20) Sugimoto, H.; Tarumizu, M.; Miyake, H.; Tsukube, H. *Eur. J. Inorg. Chem.* **2006**, 4494–4497.
(21) Sugimoto, H.; Harihara, M.; Shiro, M.; Sugimoto, K.; Tanaka, K.; Miyake, H.; Tsukube, H. *Inorg. Chem.* **2005**, *44*, 6386–6392.
(22) Schulzke, C. *Dalton Trans.* **2005**, 713–720.
(23) Hammes, B. S.; Chohan, B. S.; Hoffman, J. T.; Einwächter, S.; Carrano, C. J. *Inorg. Chem.* **2004**, *43*, 7800–7806.
(24) Hoffman, J. T.; Tran, B. L.; Carrano, C. J. *Dalton Trans.* **2006**, 3822–3830.
(25) Hoffman, J. T.; Einwächter, S.; Chohan, B. S.; Basu, P.; Carrano, C. J. *Inorg. Chem.* **2004**, *43*, 7573–7575.
(26) Venkataramanan, N. S.; Kuppuraj, G.; Rajagopal, S. *Coord. Chem. Rev.* **2005**, *249*, 1249–1268.
(27) McGarrigle, E. M.; Gilheany, D. G. *Chem. Rev.* **2005**, *105*, 1563–1602.
(28) Fürstner, A.; Leitner, A. *Angew. Chem., Int. Ed.* **2002**, *41*, 609–612.
(29) Gibson, V. C.; Spitzmesser, S. K. *Chem. Rev.* **2003**, *103*, 283–316.
(30) Williams, C. K. B. L. E.; Choi, S. K.; Nam, W.; Young, V. G.; Hillmyer, M. A.; Tolman, W. B. *J. Am. Chem. Soc.* **2003**, *125*, 11350–11359.
(31) Huang, C.-A.; Ho, C.-L.; Chen, C.-T. *Dalton Trans.* **2008**, 3502–3510.
(32) Cox, A. R. F.; Gibson, V. C.; Marshall, E. L.; White, A. J. P.; Yeldon, D. *Dalton Trans.* **2006**, 5014–5023.
(33) Marinescu, S. C.; Agapie, T.; Day, M. W.; Bercaw, J. E. *Organometallics* **2007**, *26*, 1178–1190.
(34) Binda, P. I.; Delbridge, E. E. *Dalton Trans.* **2007**, 4685–4692.
(35) Binda, P. I.; Delbridge, E. E.; Abrahamson, H. B.; Skelton, B. W. *Dalton Trans.* **2009**, 2777–2787.
(36) Hinshaw, C. J.; Peng, G.; Singh, R.; Spence, J. T.; Enemark, J.; Bruck, M.; Kristofzski, J.; Merbs, S. L.; Ortega, R. B.; Wexler, P. A. *Inorg. Chem.* **1989**, *28*, 4483–4491.
(37) Lehtonen, A.; Wasberg, M.; Sillanpää, R. *Polyhedron* **2006**, *25*, 767–775.
(38) Lehtonen, A.; Sillanpää, R. *Polyhedron* **2005**, *24*, 257–265.
(39) Wong, Y. L.; Chan, E. S. H.; Yang, Q.; Mak, T. C.; Ng, D. K. P. *J. Chem. Soc., Dalton Trans.* **1998**, 3057–3064.
(40) Thapper, A.; Behrens, A.; Fryxelius, J.; Johansson, M. H.; Prestopino, F.; Czaun, M.; Rehder, D.; Nordlander, E. *Dalton Trans.* **2005**, 3566–3571.

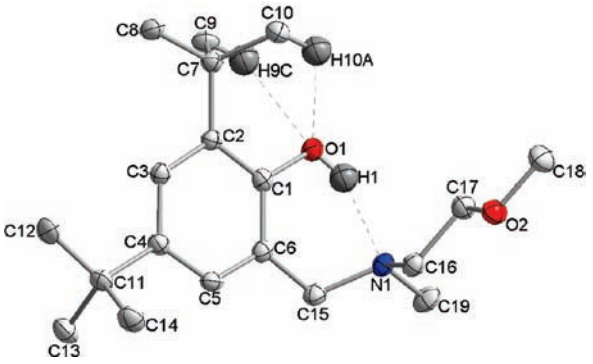

Figure 2. The molecular structure of HL^{OMe}. Hydrogen atoms have been omitted for clarity, except for those involved in hydrogen bonds. Selected bond lengths (Å) and bond angles (deg): C1−O1, 1.3690(14); C2−C7, 1.5443(16); C4−C11, 1.5350(16); C6−C15, 1.5161(17); C15−N1, 1.4768(16); N1−C16, 1.4698(16); C1−C6−C15, 120.57(11); C6−C1−O1, 119.83(10); C6−C15−N1, 113.17(10); C15−N1−C16, 111.86(9).

Scheme 1. Synthetic Procedure for the Preparation of the Phenol Ligands

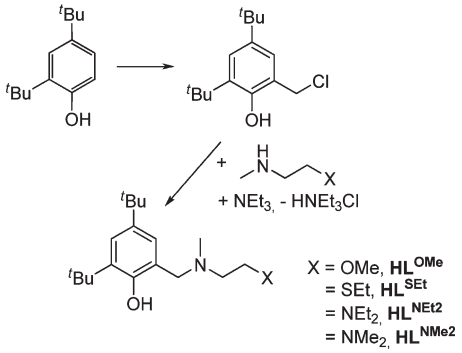

Table 1. Hydrogen Bonds in Ligand HL^{OMe}

hydrogen bonds	donor−H	H···acceptor	donor···acceptor
O1−H1···N1	0.84	1.92	2.6696
C9−H9C···O1	0.98	2.36	3.0119
C10−H10A···O1	0.98	2.33	2.9877

in the ^{1}H NMR and singlets around 60 ppm in the ^{13}C NMR spectra. Upon coordination, the two hydrogen atoms become inequivalent, giving rise to two doublets that are significantly shifted to low field (vide infra). This provides a convenient tool, allowing fast determination of coordination. Furthermore, elemental analyses and mass spectrometry confirm the formation of the targeted ligands.

Of ligand HL^{OMe}, pale yellow crystals suitable for X-ray diffraction analysis were obtained by recrystallization from dioxane. A molecular view along with selected bond lengths and angles is given in Figure 2. Crystal data show the formation of several hydrogen bonds (Table 1). The phenolic oxygen atom O1 interacts with the H9 and H10 atoms with similar distances. A strong hydrogen bond interaction of H1 with N1 leads to the local fixation of the alkyl side chain in such a way that, for subsequent coordination, little conformational change is required.

The substituent CH_2CH_2OMe at N1 is dangling in HL^{OMe} and requires rotation along several bonds for coordination (HL^{OMe}, C1−C6−C15−N1, 40.83(15); complex **2**, C6−C1−C15−N1, 50.0(17); complex **3**, C3−C2−C1−N1, 59.9(7), vide infra).

Scheme 2. Synthetic Procedure for the Preparation of the Potassium Salts of the Ligands

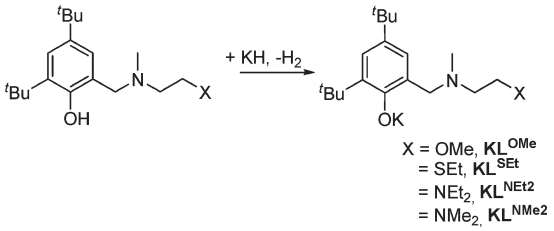

Potassium salts of the ligands were obtained by slow addition of the corresponding ligand to a slurry of potassium hydride in tetrahydrofuran at room temperature (Scheme 2). After 15 h, the reaction mixture was filtered through a pad of Celite and the solvent removed. After washing with pentane, the products were obtained in good yields as white powders and were used without further purification. They can be stored in a glovebox for an unlimited amount of time.

Slow evaporation of a concentrated benzene solution of KL^{NMe2} led to single crystals suitable for X-ray diffraction analysis. A molecular view is given in Figure 3 showing the salt exhibiting a tetrameric structure. Selected bond lengths and angles can be found in Table 2 and crystallographic data in Table 5.

The four units are arranged around a center of symmetry, leading to two crystallographically independent potassium atoms and ligands. Two potassium atoms and two phenolic oxygen atoms of the ligands form an only slightly distorted square parallelogram [K1−O1−K1′, 91.88(4)° and O1−K1−O1′, 88.12(4)°]. All four atoms deviate only by approximately 0.1 Å from a least-squares plane of K_2O_2. Potassium and phenolic oxygen atoms of the two other ligands are located on opposite sites of the square, as shown in Figure 3. All coordinating atoms within one ligand (the phenolic oxygen and two nitrogen atoms) bind to the same potassium center. Bridging occurs exclusively by the formation of K−O(phenolic)−K interactions. This leads to four- or five-coordinate potassium atoms, respectively. The central K1 atoms are coordinated by the three dentate ligands and are involved in an interaction with two additional phenolic oxygen atoms, whereas the K2 atoms are coordinated to three ligand donor atoms and only one additional oxygen atom, leading to an unusual low coordination number of four. The six-membered chelate rings have boat geometries with the phenolic oxygen and the ortho carbon being approximately coplanar with the aromatic ring.

In contrast to KL^{NMe2}, the solid-state structure of the potassium salt of a similar ligand with a $CH_2N(CH_2CH_2NEt_2)_2$ substituent in the ortho position of the phenol shows it to be dimeric.[32] The additional donor in the ligand prevents further aggregation, as found in KL^{NMe2}.

Molybdenum Dioxo Complexes. Molybdenum complexes were readily accessible by employing the η^2-coordinate pyrazolate complex [$MoO_2Cl(\eta^2$-*t*-Bu_2pz)]. The nitrogen ligand can easily be exchanged by the phenol ligands HL^{OMe}, HL^{SEt}, HL^{NEt2}, and HL^{NMe2}, leading to the monosubstituted complexes shown in Scheme 3 in

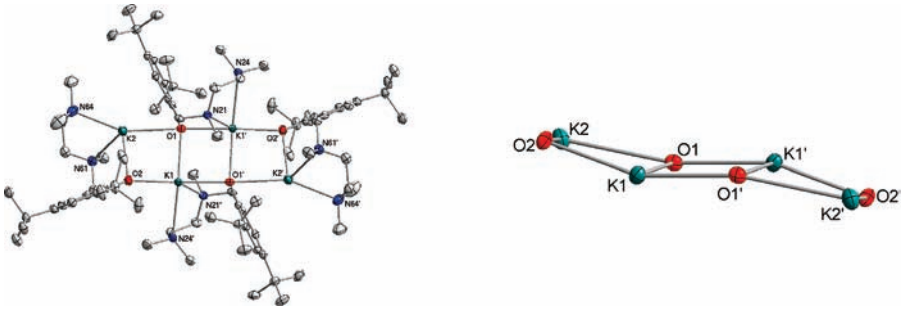

Figure 3. The molecular structure of KL^{NMe2}. The right-hand side shows the tetrameric core of the compound.

Table 2. Selected Bond Lengths (Å), Bond Angles (deg), and Torsion Angles (deg) for the Potassium Salt of the Ligand KL^{NMe2}

K1−O1	2.6699(13)	K1−N21′	2.8537(16)
K1−O2	2.6226(13)	K1−N24′	2.9100(17)
K1−O1′	2.7116(14)	K2−N61	2.8827(17)
K2−O1	3.0359(14)	K2−N64	2.8181(19)
K2−O2	2.5480(14)		
O1−K1−O1′	88.12(4)	K1−O1−K2	84.47(4)
O1−K1−O2	92.38(4)	K1−O1−K1′	91.88(4)
O2−K1−O1′	159.83(4)	K1′−O1−K2	167.24(5)
O1−K1−N21′	95.62(4)	O2−K1−N21′	126.20(5)
O1−K1−N24′	154.75(5)	O2−K1−N24′	88.85(5)
O1′−K1−N21′	73.73(4)	N21′−K1−N24′	63.96(5)
O1′−K1−N24′	99.22(4)		
O1′−K1−O1−K1′	0.0	O2−K1−O1−K1′	159.82(4)
O1′−K1−O1−K2	−167.75(5)	O2−K1−O1−K2	−7.92(4)

Scheme 3. New Synthetic Procedure for the Preparation of Molybdenum(VI) Dioxo Complexes

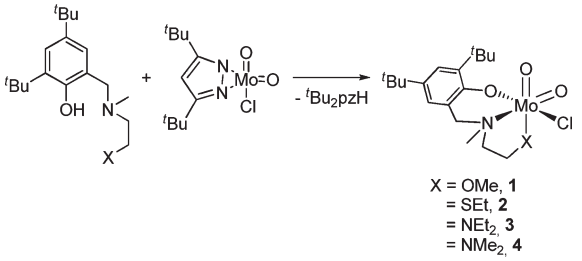

good yields. The unusual molybdenum starting material offers the advantage of short reaction times and a very easy workup procedure. After stirring the reaction mixtures for not more than 15 min, the solvent was removed, and the formed side product, bis-*tert*-butylpyrazole, was extracted from the solids with pentane, leading to the pure compounds as yellow to orange powders. Recrystallization from toluene led, for complexes **2** and **3**, to crystals suitable for X-ray diffraction analysis, showing in both cases a facially coordinated ligand with the phenol oxygen atom trans to the chlorine atom (vide infra).

Complexes **1**−**4** can also be prepared by more conventional methods employing $[MoO_2Cl_2]$ as a starting material and either potassium salts of the ligands or a mixture of HL^X and excess triethylamine, as shown in Scheme 4.

The triethyl amine method would be favorable, as it involves fewer synthetic steps. However, obtained yields and purities were, for both methods, significantly lower than when employing the molybdenum pyrazolate precursor (Table 3). In particular, the NEt_3 method proved to be difficult due to the often occurring formation of unidentified impurities, which in one case (with the HL^{NEt2} ligand) did not allow the isolation of any product. Possibly, competition between the similar added and internal bases led to polymeric materials. The general low purity of the raw products obtained by both conventional methods sometimes prevented crystallization to obtain pure products. These findings make up for the extra effort of synthesizing the precursor $[MoO_2Cl(\eta^2\text{-}t\text{-}Bu_2pz)]$.[41,42]

Scheme 4. Conventional Methods for the Preparation of Molybdenum(VI) Complexes

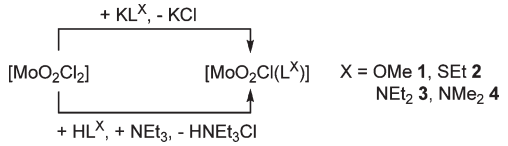

Table 3. Obtained Yields (%) of Molybdenum(VI) Dioxo Complexes Using Different Synthetic Procedures

synthetic method	complex **1**	complex **2**	complex **3**	complex **4**
$[MoO_2Cl(\eta^2\text{-}t\text{-}Bu_2pz)]/HL^X$	79	71	73	67
MoO_2Cl_2/HL^X	55	42		41
MoO_2Cl_2/KL^X	62	58	54	57

Molybdenum complexes **1**−**4** are readily soluble in common organic solvents such as THF, toluene, or benzene, but they are insoluble in alkanes. They decompose to blue intractable products in the presence of wet solvents and moist air but can be stored in a glovebox for months or weeks depending on the donor atom in the side arm. Thus, complexes with the two ligands with an additional oxygen or sulfur atom can be stored for several months, whereas those with nitrogen donor atoms decompose within four to five weeks, even in the absence of moisture and air. In particular, compound **1**, which includes a methoxy group, proved to be significantly more stable than compounds **2**−**4**. The hard oxygen donor leads to a stable chelate with the hard molybdenum(VI) atom. With only one substituent (methyl) at O, the steric demand is significantly lower than in the nitrogen analogues, explaining the stability.

The structures of the complexes in solution were investigated by ^1H and ^{13}C NMR spectroscopy. In principle, the tridentate ligands with three different donor atoms can lead to various isomers. However, for complexes **1** and **2**, only one isomer can be detected in

(41) Most, K.; Köpke, S.; Dall'Antonia, F.; Mösch-Zanetti, N. C. *Chem. Commun.* **2002**, 1676–1677.
(42) Most, K.; Hossbach, J.; Vidovic, D.; Magull, J.; Mösch-Zanetti, N. C. *Adv. Synth. Catal.* **2005**, *347*, 463–472.

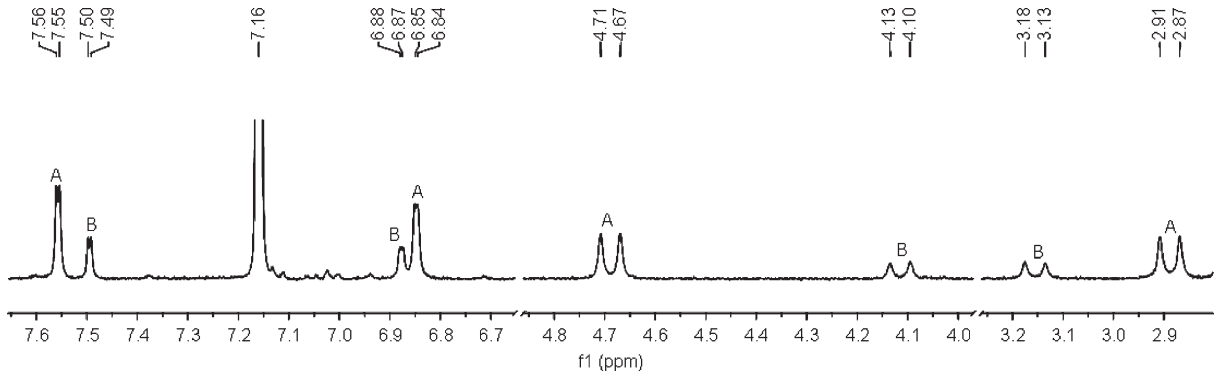

Figure 4. ^{1}H NMR spectrum in benzene-d_6 of complex **4** in the region of 7.6−2.8 ppm showing the two sets of resonances for the aromatic protons and the ortho CH_2 group (ratio isomer A/B = 3:1).

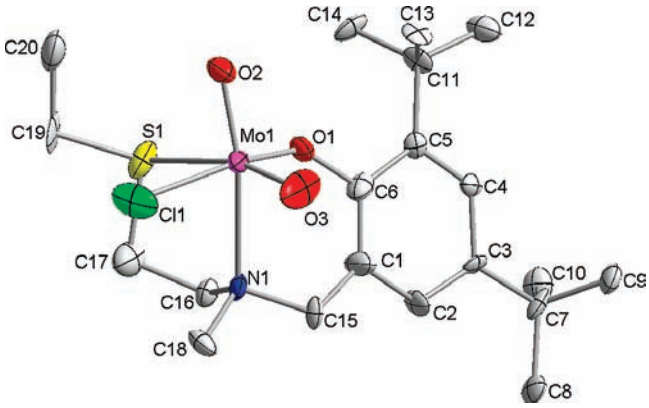

Figure 5. Molecular structure of complex **2**. Hydrogen atoms have been omitted for clarity.

solution. The two distinctive doublets for the two protons of the methylene group between the nitrogen atom and the aromatic part appear in the ^{1}H NMR spectrum for **1** at 2.95 and 4.01 ppm and for **2** at 2.90 and 4.12 ppm (Figure 4). Contrarily to the complexes employing the ligands with an additional oxygen or sulfur donor, both complexes with the nitrogen-donating arms (complexes **3** and **4**) exist as a mixture of two isomers in solution. Thus, ^{1}H and ^{13}C NMR spectroscopy reveal two sets of resonances for the respective ligand in different ratios. The ^{1}H NMR spectrum of complex **3** reveals the formation of two isomers in a 1:1 ratio and that of complex **4** in a 1:3 ratio. In the latter case, each resonance could be assigned to one or the other isomer, whereas the 1:1 ratio found in complex **3** prevented such an assignment. Presumably, the major isomer of complex **4** corresponds to the fac complex. The minor isomer is believed to be another fac compound in both compounds **3** and **4**, indicated by theoretical considerations as described below. High-temperature ^{1}H NMR spectroscopy on samples of compounds **3** and **4** between 25 and 70 °C, respectively, did not show coalescence of the resonances. This indicates that the two isomers do not interact and represent presumably two kinetic products. This would allow a separation of the isomers possibly by chromatographic means. However, the distinct sensitivity toward any traces of moisture prevented their handling on chromatographic support without decomposition.

The IR spectra of the complexes display two strong $\nu_{Mo=O}$ bands at 930 and 904 cm^{-1} for **1**; at 940 and 910 cm^{-1} for **2**; at 930, 914, 908, and 858 cm^{-1} for **3**; and at 936, 922, 906, and 856 cm^{-1} for **4**, characteristic for symmetric and asymmetric vibrational modes, respectively, of the *cis*-$[MoO_2]^{2+}$ fragment.[43,44,18]

Table 4. Selected Bond Lengths (Å), Bond Angles (deg), Torsion Angles (deg) for Complexes **2** and **3**

complex **2**		complex **3**	
Mo−O1	1.913(8)	Mo−O1	1.930(4)
Mo−O2	1.705(7)	Mo−O2	1.705(4)
Mo−O3	1.694(8)	Mo−O3	1.702(4)
Mo−N1	2.430(8)	Mo−N1	2.387(5)
Mo−S1	2.750(3)	Mo−N2	2.492(5)
Mo−Cl1	2.384(3)	Mo−Cl1	2.4172(16)
N1−C15	1.488(14)	N1−C1	1.504(7)
N1−C16	1.418(15)	N1−C17	1.496(7)
O1−C6	1.377(12)	O1−C3	1.376(6)
C1−C15	1.618(17)	C1−C2	1.499(7)
O1−Mo−Cl1	158.8(2)	O1−Mo−Cl1	162.58(11)
O2−Mo−N1	164.2(3)	O2−Mo−N1	161.80(18)
O3−Mo−O1	98.4(4)	O3−Mo−O2	107.02(19)
O3−Mo−O2	106.9(4)	O3−Mo−N2	165.76(17)
O3−Mo−S1	162.9(3)	N1−Mo−N2	75.01(15)
N1−C15−C1	110.2(10)	C2−C1−N1	115.9(4)
C2−C1−C6-O1	175.8(11)	C1−C2−C7−C6	167.8(5)
C15−C1−C6-C5	157.9(11)	C7−C2−C3−O1	178.8(5)

Molecular Structure in the Solid State. Single crystals suitable for X-ray diffraction analysis of complex **2** were obtained from a concentrated benzene solution. A molecular view is shown in Figure 5. Selected bond lengths and angles are given in Table 4 and crystallographic data in Table 5. The X-ray structure of complex **2** reveals a six-coordinate Mo atom in a distorted octahedral surrounding, with a fac coordination of the ligand. The phenol oxygen atom is located trans to the chlorine atom. The molybdenum oxo groups show the expected mutual cis configuration with a trans amino and a trans thioether ligand, respectively. The Mo−O bond lengths (Mo−O1, 1.913(8) Å), the Mo═O bond lengths (Mo−O2, 1.705(7) Å; Mo−O3, 1.694(8) Å), and the Mo−Cl bond lengths (Mo−Cl, 2.384(3) Å) are in the expected range of cis-dioxo Mo^{VI} complexes.[18,45,46] The trans influence of the terminal oxygen atoms O2 and O3 lengthens the Mo−N bond (Mo−N1, 2.430(8) Å) and the

(43) Schultz, B. E.; Gheller, S. F.; Muetterties, M. C.; Scott, M. J.; Holm, R. H. *J. Am. Chem. Soc.* **1993**, *115*, 2741–2722.
(44) Thomson, L. M.; Hall, M. B. *J. Am. Chem. Soc.* **2001**, *123*, 3995–4002.
(45) Lyashenko, G.; Herbst-Irmer, R.; Jancik, V.; Pal, A.; Mösch-Zanetti, N. C. *Inorg. Chem.* **2008**, *47*, 113–120.
(46) Tran, B. L.; Carrano, C. J. *Inorg. Chem.* **2007**, *46*, 5429–5438.

Table 5. Crystal Data, Data Collection, and Refinement Parameters for Compounds HL^{OMe} and KL^{NMe2}, Complex **2**, and Complex **3**

	HL^{OMe}	KL^{NMe2}	complex **2**	complex **3**
empirical formula	$C_{19}H_{33}NO_2$	$(C_{20}H_{35}KN_2O)_4$	$C_{20}H_{34}ClMoNO_3S$	$C_{22}H_{39}ClMoN_2O_3$
fw	307.46	1434.40	500.01	511.02
temp	100(2) K	95K	100(2) K	100(2) K
wavelength	0.71073 Å	0.71069 Å	0.71073 Å	0.71073 Å
cryst syst, space group	monoclinic, $P2(1)/c$	monoclinic, $P2(1)/c$	monoclinic, $P2(1)$	monoclinic, $P2(1)/c$
unit cell dimensions	a = 6.1149(12) Å	19.046(3)Å	a = 10.330(2) Å	a = 14.701(3) Å
	α = 90°		α = 90°	α = 90°
	b = 18.279(4) Å	18.085(3)Å	b = 11.243(2) Å	b = 13.314(3) Å
	β = 92.34(3)°	110.818(13)°	β = 108.19(3)°	β = 97.63(3)°
	c = 16.726(3) Å	13.499(2)Å	c = 14.653(3) Å	c = 18.667(4) Å
	γ = 90°		γ = 90°	γ = 90°
volume	1868.0(6) $Å^3$	4346.1(12)$Å^3$	1616.8(6) $Å^3$	3621.4(13) $Å^3$
Z, calculated density	4, 1.093 Mg/m^3	2, 1.096Mg/m^3	2, 1.348 Mg/m^3	4, 1.295 Mg/m^3
abs coeff	0.069 mm^{-1}	0.253 mm^{-1}	0.584 mm^{-1}	0.472 mm^{-1}
F(000)	680	1568	688	1492
cryst size	0.45 × 0.36 × 0.28 mm	0.40 × 0.32 × 0.28 mm	0.34 × 0.20 × 0.18 mm	0.38 × 0.28 × 0.24 mm
θ range for data collection	1.65−26.37°	2.53−26.00°	2.08−25.00°	1.40−26.32°
limiting indices	$-7 \le h \le +7$	$-23 \le h \le +22$	$-12 \le h \le +12$	$-18 \le h \le +18$
	$-22 \le k \le +22$	$-1 \le k \le +22$	$-13 \le k \le +13$	$-16 \le k \le +16$
	$-20 \le l \le +20$	$-1 \le l \le +16$	$-17 \le l \le +17$	$-23 \le l \le +23$
reflns collected/unique	14439/3817	10238/8508	11658/5619	28330/7350
	[R(int) = 0.0249]	[R(int) = 0.0325]	[R(int) = 0.0928]	[R(int) = 0.0792]
completeness to θ = 25.00	99.8%	99.6%	99.9%	99.6%
abs corrn	SADABS	empirical	SADABS	SADABS
refinement method	full-matrix least-squares on F^2	full-matrix least-squares on F^2	full-matrix least-squares on F^2	full-matrix least-squares on F^2
data/restraints/params	3817/0/208	8508/490/0	5619/55/390	7350/0/406
goodness-of-fit on F^2	1.054	1.020	1.091	1.306
final R indices [I > 2σ(I)]	R1 = 0.0439	R1 = 0.0439	R1 = 0.0870	R1 = 0.0897
	wR2 = 0.1144	wR2 = 0.0981	wR2 = 0.1554	wR2 = 0.1707
R indices (all data)	R1 = 0.0471	R1 = 0.0601	R1 = 0.1108	R1 = 0.1037
	wR2 = 0.1167	wR2 = 0.1072	wR2 = 0.1667	wR2 = 0.1761
largest diff. peak and hole	0.315 and −0.204 e/$Å^{-3}$	0.348 and −0.336 e/$Å^3$	1.055 and −1.597 e/A^{-3}	1.674 and −2.030 e/A^{-3}

Mo−S bond (Mo−S1, 2.750(3) Å).[46−48,36,49] Furthermore, the phenolic O1 atom and the C15 atom are nonplanar to the benzene ring, which is indicated by the obtuse torsion angles C2−C1−C6−O1 (175.8(11)°) and C15−C1−C6−C5 (157.9(11)°).

Single crystals of compound **3** suitable for X-ray diffraction analysis were obtained from a concentrated benzene solution at room temperature. Characterization of this compound in solution revealed two isomers. In contrast to this, only one type of crystal could be detected in several crystallizing samples, indicating that the second isomer has poorer crystallizing capabilities.

The molecular structure of complex **3** is comparable to that of complex **2** (a molecular view is shown in Figure 6). Both compounds reveal a six-coordinate distorted octahedral geometry with a facial coordination of the ligand. All bond lengths are comparable in both complexes. The different trans influences of the additional donors (SEt in **2** versus NEt_2 in **3**) have little effect on the bond lengths of the trans Mo=O group (Mo−O3 1.694(8) Å in complex **2** versus Mo−O3 1.702(4) Å in complex **3**). However, slightly longer is the Mo−Cl bond in **3** (Mo1−Cl1, 2.4172(16) Å), in comparison to complex **2** (Mo1−Cl1, 2.384(3) Å).

OAT Reactions. The ability of complex **1** to transfer an oxygen atom has been investigated using PMe_3 as the substrate. An immediate reaction was obvious as a color change from yellow to brown. The reaction was monitored via ^{31}P NMR spectroscopy, showing the formation of $OPMe_3$. However, the ^{31}P NMR spectra revealed additionally the formation of a known molybdenum complex, *cis*,*mer*-$[MoOCl_2(PMe_3)_3]$, indicated by a triplet at −2.31 ppm and a doublet at −8.76 ppm.[50,51] Further evidence for the formation of *cis*,*mer*-$[MoOCl_2(PMe_3)_3]$ provides the ^1H NMR spectrum, showing a pseudo triplet at 1.39 ppm due to the two *trans*-PMe_3 ligands and a doublet at 1.28 ppm due to the single *cis*-PMe_3 ligand, which is in agreement with the literature data. Next to these, the proton NMR spectrum shows the resonances for the free ligand. Thus, it seems likely that oxygen atom transfer from the dioxo complex **1** to phosphorus occurred, but the presumed reduced complex $[MoOClL^{OMe}]$ is not stable toward ligand L^{OMe} dissociation. The driving force for the formation of *cis*,*mer*-$[MoOCl_2(PMe_3)_3]$ is possibly its high stability. Therefore, we are currently investigating the substitution of the remaining chlorine ligand, thereby preventing its formation.

Theoretical Calculations. With the prerequisite that, in all complexes, a *cis*-MoO_2 arrangement is the most stable geometry, in principle, the formation of five different diastereoisomeric (and 10 enantiomeric) molybdenum complexes is conceivable. With the internal NMe moiety in the R configuration, there exist three fac isomers with the Cl ligand being coordinated either trans to the phenolate oxygen atom, trans to the internal N atom, or trans to the terminal donor atom (N, O, or S) and two mer

(47) Doonan, C. J.; Millar, A. J.; Nielsen, D. J.; Young, C. G. *Inorg. Chem.* **2005**, *44*, 4506–4515.
(48) Berg, J. M.; Holm, R. H. *J. Am. Chem. Soc.* **1985**, *107*, 925–932.
(49) Xiao, Z.; Young, C. G.; Enemark, J.; Wedd, A. G. *J. Am. Chem. Soc.* **1992**, *114*, 9194–9195.
(50) Yoon, K.; Parkin, G.; Rheingold, A. L. *J. Am. Chem. Soc.* **1992**, *114*, 2210–2218.
(51) Limberg, C.; Büchner, M.; Heinze, K.; Walter, O. *Inorg. Chem.* **1997**, *36*, 872–879.

isomers where the Cl ligand is in a trans position to an oxo ligand, where the internal NMe moiety adopts either an R or a S configuration. The optimized geometries and relative free energies of all diastereomeric molybdenum complexes with the different tridentate ligands, namely, L^{NMe2}, L^{OMe}, and L^{SMe}, have been established by DFT calculations. The relative energies and optimized geometries for the complexes with the L^{NMe2} ligand are depicted in Figure 7. The results for the other two ligand systems are given in the Supporting Information (Figures S1 and S2).

For the ligand L^{NMe2}, calculations reveal that the facial complexes **C1** and **C3**, where the Cl atom is in a trans position to the phenolate oxygen atom and trans to the terminal NMe_2 moiety, respectively, are the most stable isomers exhibiting similar relative free energies (Figure 7). In the case of the ligands L^{OMe} and L^{SMe}, the thermodynamically most stable compounds are $\mathbf{C1}^{\mathbf{OMe}}$ and $\mathbf{C1}^{\mathbf{SMe}}$, where the tridentate ligand adopts a facial geometry with the Cl ligand lying trans to the phenolate oxygen atom.

However, the energy differences of all isomers are comparatively small, particularly in the case of the three fac isomers, suggesting that the formation of the molybdenum complexes is kinetically rather than thermodynamically controlled. Experimentally, with the L^{OMe} and L^{SMe} ligands, exclusively, one facial isomer is formed and both are unequivocally characterized by solution NMR and X-ray crystallography (for L^{SMe}). These compounds correspond to the two thermodynamically most stable complexes $\mathbf{C1}^{\mathbf{OMe}}$ and $\mathbf{C1}^{\mathbf{SMe}}$. With the L^{NMe2} ligand, however, in solution, two isomers are formed. In the solid state, one of these could be crystallographically characterized, which corresponds to the calculated fac isomer **C1** (Figure 7).

This prompted us to investigate in detail the mechanism of the formation of *cis*-molybdenum dioxo complexes. As a model, we have chosen the $[MoO_2Cl(L^{NMe2})]$ system. Along these lines, several pathways and key intermediates can be proposed, and these are depicted in Figures 7−10 (free energies in kilocalories per mole). Upon treatment of $[MoO_2Cl_2]$ with the deprotonated ligand L^{NMe2} (arbitrarily chosen with an S configuration at the internal N atom), it is most likely that the tetrahedral intermediates **A1** and **A3** are initially formed (Figures 8−10).

In these intermediates, the strongly basic phenolic oxygen atom is coordinated, while the pendant $-CH_2NMeCH_2CH_2NMe_2$ arm remains uncoordinated, being either cis or trans to the Cl ligand. Subsequent coordination of the internal NMe moiety leads to the pentacoordinated intermediates **B1**, **B2**, and **B3** (it has to

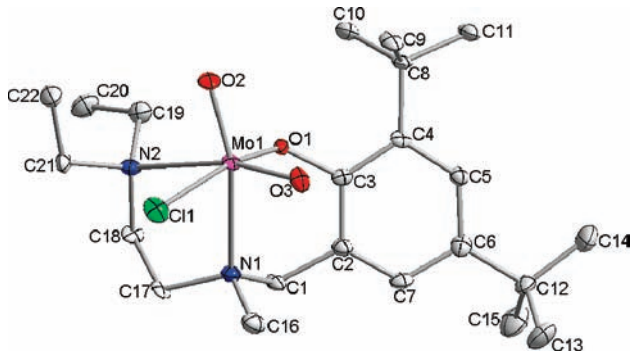

Figure 6. Molecular structure of complex **3**. Hydrogen atoms have been omitted for clarity.

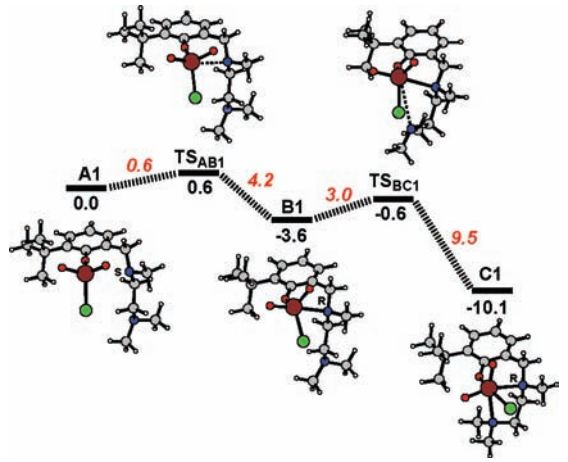

Figure 8. Profile of the B3LYP potential energy surfaces (free energies in kcal/mol) for the conversion of **A1** to the fac isomer **C1** where the internal NMe moiety adopts an R configuration.

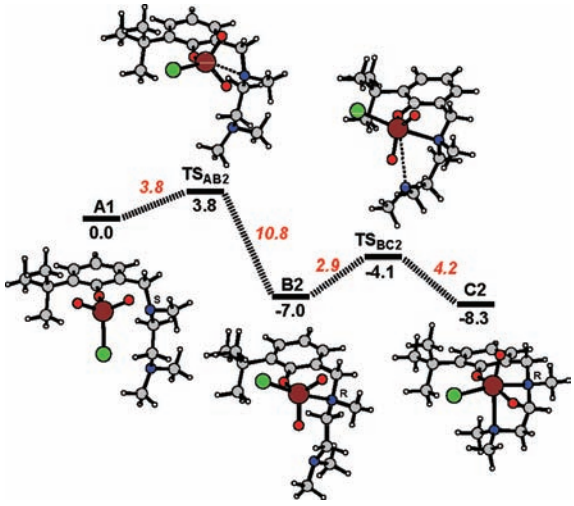

Figure 9. Profile of the B3LYP potential energy surfaces (free energies in kcal/mol) for the conversion of **A1** to the fac isomer **C2** where the internal NMe moiety adopts an R configuration.

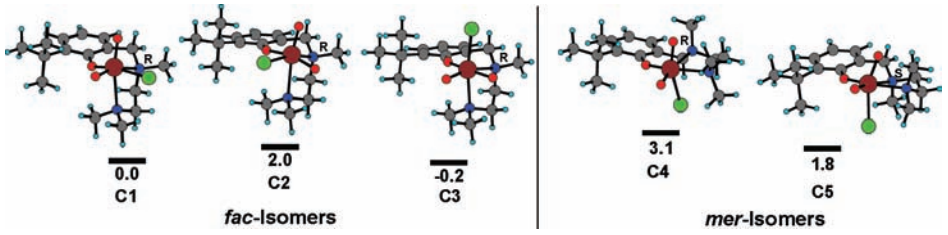

Figure 7. Optimized geometries and relative free energies (in kcal/mol) with facial and meridional geometries of the tridentate ligand L^{NMe2} calculated at the B3LYP level of theory (Mo sdd; C, N, H, O, Cl H 6-31 g**).

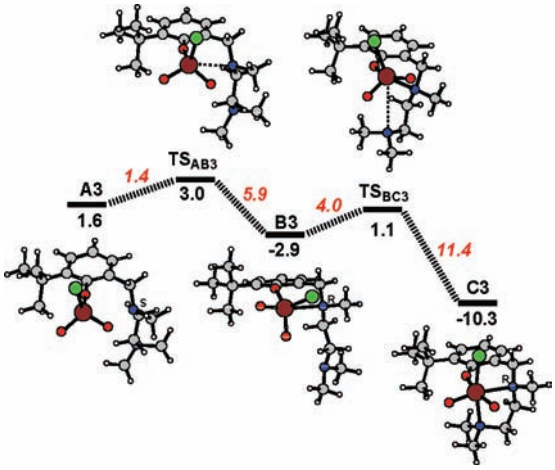

Figure 10. Profile of the B3LYP potential energy surfaces (free energies in kcal/mol) for the conversion of **A3** to the fac isomer **C3** where the internal NMe moiety adopts an R configuration.

be noted that the internal NMe moiety adopts now an R configuration due to priority rules). The free energies of activation for these intramolecular processes are small, being 0.6, 3.8, and 1.4 kcal/mol, respectively. The two possible mer isomers are formed in a similar fashion (see the Suppoting Information, Figures S3 and S4) with barriers of 3.1 and 3.8 kcal/mol. The formation of **B1** and **B3** is kinetically strongly favored over **B2**, **B4**, and **B5**, which corresponds to relative first-order rate constants of 222.8 (**B1**), 57.6 (**B3**), 3.3 (**B5**), and 1 (**B2**, **B4**). Accordingly, **B1** and **B3** should be formed roughly in a 3.9:1 ratio, which agrees fairly well with the experimental value of 3:1 for complex **4**. Finally, upon coordination of the terminal NMe_2 unit, the products **C1**−**C5** are formed.

The energy barrier for the last step is typically lower for the fac than for the mer isomers. The overall reactions are, in all cases, exergonic by about 7.0 to 10.3 kcal/mol. Thus, on the basis of DFT calculations, it is most likely that the formation of the fac isomers **C1** and **C3** is strongly favored on kinetic rather than thermodynamic grounds.

It has to be mentioned that the formation of mer isomers **C4** and **C5** can also be excluded on the basis of gauge-independent atomic orbital (GIAO) calculations of the proton NMR shifts of complexes **C1**−**C5**. These compounds exhibit typically distinctive signals for the two protons of the methylene group between the nitrogen atom and the aromatic ring. Experimentally, the major isomer exhibits two signals at 4.69 and 2.89 ppm; the minor one gives rise to signals at 4.12 and 3.17 ppm. While the calculated proton NMR signals of the methylene moiety of the fac complexes **C1**−**C3** are in a similar shift range to that of the experimental ones (**C1**, 4.94/3.00 ppm; **C2**, 4.40/2.93 ppm; **C3**, 4.69/2.94 ppm), an unequivocal distinction of what facial isomer is present cannot be made. In the case of the mer complexes **C4** and **C5**, however, the calculated resonances are quite different from those of the experimental values, being 5.70/2.67 ppm and 5.59/2.56 ppm, respectively. These are less likely.

Conclusion

We were able to prepare a series of novel molybdenum(VI) dioxo complexes with tridentate phenolate ligands using the uncommon η^2-coordinated [$MoO_2Cl(\eta^2$-*t*-Bu_2pz)] complex as a starting material. All complexes were readily accessible in pure forms and good yields by substituting the *t*-Bu_2pz moiety with the new ligands. Depending on the donor atom of the alkyl chain, we obtained isomerically pure compounds (complexes **1** and **2**), or a mixture of two isomers in solution (complexes **3** and **4**). X-ray diffraction analysis showed the ligand to be, in all cases, facially coordinated. High-temperature ^{1}H NMR spectroscopy as well as theoretical calculations indicate the formation of two facially coordinated isomers on kinetic grounds. Oxygen atom transfer from **1** to phosphorus is fast but leads to the formation of *cis*,*mer*-[$MoOCl_2(PMe_3)_3$]. Possibly, high flexibility of the ethylene-based donors led to a reduced chelate effect, enabling substitution of the ligand. We are currently investigating substitution reactions of Cl at molybdenum, preventing the formation of [$MoOCl_2(PMe_3)_3$].

Experimental Section

General Remarks. All reactions involving air-sensitive compounds were carried out under an atmosphere of dry argon using either Schlenk techniques or a glovebox. All solvents besides benzene-d_6, THF-d_8, and dioxane were dried over sodium/potassium alloy under argon or purified via a Pure Solv MD-4-EN solvent purification system from Innovative Technology, Inc. Dioxane was dried over aluminum oxide and distilled prior to use. Celite and aluminum oxide were purchased from commercial sources and dried in vacuo at 300 °C. [MoO_2Cl_2] was purchased from Adrich. All other chemicals were obtained from different suppliers and used without further purification. The following compounds were prepared following published procedures: 2-hydroxy-3,5-di-*tert*-butylbenzylchloride,[52] N-methyl-[(2-ethylsulfanyl)ethyl]-amine,[53] 4,6-di-*tert*-butyl-6-{[(2′-methoxy-ethyl)methylamino]methyl}phenol,[31] 4,6-di-*tert*-butyl-6-{[(2′-dimethylaminoethyl)methyl-amino]-methyl}phenol,[30] and [$MoO_2Cl(\eta^2$-3,5-di-*tert*-butyl-pyrazolate)].[41,42]

All ^{1}H and ^{13}C NMR spectra were recorded at 360 MHz on a Bruker AMX 360 spectrometer. Chemical shift values are given in parts per million. All deuterated solvents were purchased from Deutero GmbH and dried over a molecular sieve. Mass spectra have been measured on an Agilent 5973 MSD-Direct Probe using the electrospray ionization technique. Elemental analyses were carried out using a Heraeus Vario Elementar automatic analyzer at the Institute of Inorganic Chemistry at the University of Technology in Graz, Austria. UV−vis absorption spectra were recorded on a Varian 50 Conc. UV−visible spectrophotometer. IR spectra were recorded with a Perkin-Elmer 1725 X FT-IR spectrometer.

4,6-Di-*tert*-butyl-2-{[(2′-methoxyethyl)methylamino]methyl}-phenol (HL^{OMe}). Ligand HL^{OMe} is already known in the

(52) Abufarag, A.; Vahrenkamp, H. *Inorg. Chem.* **1995**, *34*, 3279–3284.
(53) Frisch, M. J.; Trucks, G. W.; Schlegel, H. B.; Scuseria, G. E.; Robb, M. A.; Cheeseman, J. R.; Montgomery, J. J. A.; Vreven, T.; Kudin, K. N.; Burant, J. C.; Millam, J. M.; Iyengar, S. S.; Tomasi, J.; Barone, V.; Mennucci, B.; Cossi, M.; Scalmani, G.; Rega, N.; Petersson, G. A.; Nakatsuji, H.; Hada, M.; Ehara, M.; Toyota, K.; Fukuda, R.; Hasegawa, J.; Ishida, M.; Nakajima, T.; Honda, Y.; Kitao, O.; Nakai, H.; Klene, M.; Li, X.; Knox, J. E.; Hratchian, H. P.; Cross, J. B.; Bakken, V.; Adamo, C.; Jaramillo, J.; Gomperts, R.; Stratmann, R. E.; Yazyev, O.; Austin, A. J.; Cammi, R.; Pomelli, C.; Ochterski, J. W.; Ayala, P. Y.; Morokuma, K.; Voth, G. A.; Salvador, P.; Dannenberg, J. J.; Zakrzewski, V. G.; Dapprich, S.; Daniels, A. D.; Strain, M. C.; Farkas, O.; Malick, D. K.; Rabuck, A. D.; Raghavachari, K.; Foresman, J. B.; Ortiz, J. V.; Cui, Q.; Baboul, A. G.; Clifford, S.; Cioslowski, J.; Stefanov, B. B.; Liu, G.; Liashenko, A.; Piskorz, P.; Komaromi, I.; Martin, R. L.; Fox, D. J.; Keith, T.; Al-Laham, M. A.; Peng, C. Y.; Nanayakkara, A.; Challacombe, M.; Gill, P. M. W.; Johnson, B.; Chen, W.; Wong, M. W.; Gonzalez, C.; Pople, J. A. *Gaussian 03*, revision C.02; Gaussian, Inc.: Wallingford, CT, 2004.

literature,[31] but herein we used an improved synthesis for the preparation of the ligand L^{OMe}, affording the ligand in higher yields. To a solution of 2-hydroxy-3,5-di-*tert*-butylbenzylchloride (2.39 g, 9.37 mmol) in 40 mL of dioxane was added a solution of N-methyl-(2-methoxy)ethylamine (0.87 g, 9.4 mmol) in 30 mL of dioxane. The solution changed color to pale yellow. After stirring for 5 min, NEt_3 (2.8 mL, 20 mmol) was added, and a white precipitate was formed. The mixture was stirred overnight, and then, the solution was filtered over a pad of Celite. The volatiles were removed under reduced pressure to afford a yellow viscous oil, which was used without further purification. Yield: 2.40 g (83%). Crystals suitable for X-ray diffraction analysis were grown from a concentrated dioxane solution.

4,6-Di-*tert*-butyl-2-{[(2′-ethylthioethyl)methylamino]methyl}-phenol (HL^{SEt}). Synthesis of the ligand HL^{SEt} followed the method described above. To a solution of 2-hydroxy-3,5-di-*tert*-butylbenzylchloride (2.55 g, 10 mmol) in 40 mL dioxane was added a solution of N-methyl-[(2-ethylsulfanyl)ethyl]amine (1.19 g, 10 mmol) in 30 mL of dioxane. After the workup, the ligand L^{SEt} remained as a brown oil. Yield: 3.14 g (93%). ^{1}H NMR (360 MHz, benzene-d_6): δ 0.99 (t, $^3J_{H-H}$ = 7.4 Hz, 3H, SCH_2CH_3), 1.36 (s, 9H, $C(CH_3)_3$), 1.71 (s, 9H, $C(CH_3)_3$), 1.82 (s, 3H, NCH_3), 2.15 (q, $^3J_{H-H}$ = 7.4 Hz, 2H, SCH_2CH_3), 2.30 (s, 4H, NCH_2CH_2S), 3.30 (s, 2H, Ar−CH_2N), 6.88 (d, $^4J_{H-H}$ = 2.4 Hz, 1H, Ar−*H*), 7.50 (d, $^4J_{H-H}$ = 2.4 Hz, 1H, Ar−*H*). ^{13}C NMR (360 MHz, benzene-d_6): δ 15.3 (SCH_2CH_3), 26.5 (SCH_2CH_3), 29.3 (NCH_2CH_2S), 30.4 ($C(CH_3)_3$), 32.4 ($C(CH_3)_3$), 34.7 ($C(CH_3)_3$), 35.7 ($C(CH_3)_3$), 41.1 (NCH_3), 56.8 (NCH_2CH_2S), 62.6 (Ar−CH_2N), 122.0 (*Ar*), 122.1 (*Ar*), 123.5 (*Ar*), 136.4 (*Ar*), 141.0 (*Ar*), 155.4 (*Ar*−OH). MS (EI) (70 eV) *m*/*z* (%): 337 (50) [M^+], 262 (86) [$M^+ - CH_3CH_2SCH_2$], 219 (100) [$M^+ - (CH_3)_2(CH_2)_3NS$], 89 (30) [$CH_3CH_2SCH_2CH_2^+$]. Anal. Calcd for $C_{20}H_{35}NSO$: C, 71.46; H, 10.46; N, 4.15. Found: C, 70.38; H, 10.10; N, 4.56%.

4,6-Di-*tert*-butyl-2-{[(2′-diethylaminoethyl)methylamino]methyl}-phenol (HL^{NEt2}). The ligand HL^{NEt2} was prepared in an analogous manner to the ligand HL^{OMe} using a solution of 2-hydroxy-3,5-di-*tert*-butylbenzylchloride (0.53 g, 2.1 mmol) in 10 mL of dioxane and a solution of N,N-diethyl-N′-methylethylenediamine (0.27 g, 2.1 mmol) in 10 mL of dioxane. The product was obtained as a brown viscous oil, which was used without further purification. Yield: 0.67 g (91%).

^{1}H NMR (360 MHz, benzene-d_6): δ 0.91 (t, $^3J_{H-H}$ = 6.69 Hz, 6H, NCH_2CH_3), 1.38 (s, 9H, $C(CH_3)_3$), 1.73 (s, 9H, $C(CH_3)_3$), 1.97 (s, 3H, NCH_3), 2.31 (m, 8H, NCH_2), 3.40 (s, 2H, Ar−CH_2N), 6.95 (d, $^4J_{H-H}$ = 2.35 Hz, 1H, Ar−*H*), 7.52 (d, $^4J_{H-H}$ = 2.41 Hz, 1H, Ar−*H*). ^{13}C NMR (360 MHz, benzene-d_6): δ 12.3 (NCH_2CH_3), 30.4 ($C(CH_3)_3$), 32.4 ($C(CH_3)_3$), 34.7 ($C(CH_3)_3$), 35.7 ($C(CH_3)_3$), 42.0 (NCH_2CH_3), 47.6 (NCH_3), 51.2 (NCH_2CH_2N), 55.2 (NCH_2CH_2N), 62.2 (Ar−CH_2N), 122.7 (*Ar*), 123.4 (*Ar*), 124.1 (*Ar*), 136.4 (*Ar*), 140.8 (*Ar*), 155.6 (*Ar*−OH). MS (EI) (70 ev) *m*/*z* (%): 348 (60) [M^+], 262 (84) [$M^+ - (CH_3CH_2)_2NCH_2$], 219 (100) [$C_{15}H_{23}O^+$], 86 (80) [$(CH_3CH_2)_2NCH_2^+$]. Anal. Calcd for $C_{22}H_{40}N_2O$: C, 75.79; H, 11.57; N, 8.04. Found: C, 75.50; H, 11.40; N, 8.01%.

4,6-Di-*tert*-butyl-2-{[(2′-dimethylaminoethyl)methylamino]-methyl}phenol (HL^{NMe2}). Ligand HL^{NMe2} is already known in the literature,[30] but herein we describe an improved method for its preparation in higher yields. Synthesis of the ligand HL^{NMe2} followed the method described above. To a solution of 2-hydroxy-3,5-di-*tert*-butylbenzylchloride (2.63 g, 10 mmol) in 40 mL of dioxane was added a solution of N,N,N′-trimethylethylenediamine (1.06 g, 10 mmol) in 30 mL of dioxane. After the workup, the ligand L^{NMe2} was obtained as a white solid. Yield: 2.78 g (84%).

General Synthetic Procedures for Potassium Salts of Ligands KL^{OMe}, KL^{SEt}, KL^{NEt2}, and KL^{NMe2}. To a stirring slurry of 1.6 equiv of potassium hydride in 30 mL of THF was slowly added at room temperature 1 equiv of the relevant ligand dissolved in 30 mL of THF. The mixture was stirred overnight, and excess potassium hydride was filtered through a pad of Celite. The clear solution was concentrated in a vacuum to give a waxy solid. The residue was washed several times with pentane to afford the potassium salt of the ligand as a powder.

Potassium 4,6-Di-*tert*-butyl-2-{[(2′-methoxyethyl)methylamino]-methyl}phenoxide (KL^{OMe}). Synthesis of the potassium salt KL^{OMe} followed the method described above. To a solution of potassium hydride (0.20 g, 5.1 mmol) in 30 mL of THF was added a solution of the ligand L^{OMe} (0.98 g, 3.2 mmol) in 30 mL of THF. After the workup, the product remained as a light yellow powder. Yield: 0.85 g (77%). ^{1}H NMR (360 MHz, THF-d_8): δ 1.25 (s, 9H, $C(CH_3)_3$), 1.48 (s, 9H, $C(CH_3)_3$), 2.24 (s, 3H, NCH_3), 2.59 (s, 2H, NCH_2CH_2O), 3.07 (s, 3H, OCH_3), 3.38 (s, 2H, NCH_2CH_2O), 3.42 (s, 2H, Ar−CH_2N), 6.76 (s, 1H, Ar−*H*), 7.03 (s, 1H, Ar−*H*). ^{13}C NMR (360 MHz, THF-d_8): δ 30.8 ($C(CH_3)_3$), 32.9 ($C(CH_3)_3$), 34.3 ($C(CH_3)_3$), 36.1 ($C(CH_3)_3$), 41.6 (NCH_3), 57.4 (NCH_2CH_2O), 58.9 (OCH_3), 63.9 (Ar−CH_2N), 70.6 (NCH_2CH_2O), 123.0 (*Ar*), 124.5 (*Ar*), 127.9 (*Ar*), 128.2 (*Ar*), 136.5 (*Ar*), 175.0 (*Ar*−OK). Anal. Calcd for $C_{19}H_{32}NO_2K$: C, 66.10; H, 9.33; N, 4.05. Found: C, 65.97; H, 9.35; N, 4.27%.

Potassium 4,6-Di-*tert*-butyl-2-{[(2′-ethylthioethyl)methylamino]-methyl}phenoxide (KL^{SEt}). The potassium salt KL^{SEt} was prepared in an analogous manner to that described above using a THF solution of the potassium hydride (0.17 g, 4.3 mmol) and the ligand L^{SEt} (0.90 g, 2.7 mmol) in THF. After the workup and purification, KL^{SEt} was obtained as a white powder. Yield: 0.70 g (70%). ^{1}H NMR (360 MHz, benzene-d_6): δ 0.86 (t, $^3J_{H-H}$ = 7.17 Hz, 3H, SCH_2CH_3), 1.50 (s, 9H, $C(CH_3)_3$), 1.69 (s, 9H, $C(CH_3)_3$), 1.86 (q, $^3J_{H-H}$ = 7.25 Hz, 2H, SCH_2CH_3), 2.19 (s, 3H, NCH_3), 2.25 (t, $^3J_{H-H}$ = 5.41 Hz, 2H, NCH_2CH_2S), 2.45 (s, 2H, NCH_2CH_2S), 3.50 (s, 2H, Ar−CH_2N), 7.10 (s, 1H, Ar−*H*), 7.50 (d, $^4J_{H-H}$ = 2.29 Hz, 1H, Ar−*H*). ^{13}C NMR (360 MHz, benzene-d_6): δ 15.1 (SCH_2CH_3), 25.4 (SCH_2CH_3), 29.5 (NCH_2CH_2S), 30.7 ($C(CH_3)_3$), 32.8 ($C(CH_3)_3$), 34.2 ($C(CH_3)_3$), 36.0 ($C(CH_3)_3$), 43.0 (NCH_3), 55.2 (NCH_2CH_2S), 62.8 (Ar−CH_2N), 123.1 (2 × *Ar*), 124.3 (*Ar*), 128.9 (*Ar*), 136.5 (*Ar*), 167.9 (*Ar*−OK). Anal. Calcd for $C_{20}H_{34}NOSK$: C, 63.95; H, 9.12; N, 3.73. Found: C, 63.78; H, 9.07; N, 3.70%.

Potassium 4,6-Di-*tert*-butyl-2-{[(2′-diethylaminoethyl)methylamino]methyl}phenoxide (KL^{NEt2}). Synthesis of the potassium salt KL^{NEt2} followed the procedure described above. To a solution of potassium hydride (0.21 g, 5.3 mmol) in 30 mL of THF was added a solution of L^{NEt2} (1.2 g, 3.3 mmol) in 30 mL of THF. The product KL^{NEt2} was obtained as a white powdery solid. Yield: 0.88 g (68%). ^{1}H NMR (360 MHz, THF-d_8,): δ 0.84 (s, 6H, $N(CH_2CH_3)_2$), 1.24 (s, 9H, $C(CH_3)_3$), 1.45 (s, 9H, $C(CH_3)_3$), 2.37 (s, 7H, $N(CH_2CH_3)_2$, NCH_3), 2.48 (s, 4H, NCH_2CH_2N), 3.40 (s, 2H, Ar−CH_2N), 6.78 (d, $^4J_{H-H}$ = 2.41 Hz, 1H, Ar−*H*), 7.03 (d, $^4J_{H-H}$ = 2.38 Hz, 1H, Ar−*H*). ^{13}C NMR (360 MHz, benzene-d_6): δ 10.7 (NCH_2CH_3), 30.8 ($C(CH_3)_3$), 32.8 ($C(CH_3)_3$), 34.4 ($C(CH_3)_3$), 36.0 ($C(CH_3)_3$), 44.1 (NCH_2CH_2N), 46.1 (NCH_3), 50.9 (NCH_2CH_3), 51.8 (NCH_2CH_2N), 63.0 (Ar−CH_2N), 123.4 (2 × *Ar*), 124.7 (*Ar*), 129.9 (*Ar*), 136.6 (*Ar*), 167.3 (*Ar*−OK). Anal. Calcd for $C_{22}H_{39}N_2OK$: C, 68.38; H, 10.17; N, 7.25. Found: C, 68.34; H, 10.16; N, 7.62%.

Potassium 4,6-Di-*tert*-butyl-2-{[(2′-dimethylaminoethyl)methylamino]methyl}phenoxide (KL^{NMe2}). The preparation of the potassium salt of KL^{NMe2} followed the general procedure described above, using a THF solution of potassium hydride (0.2 g, 5 mmol) and a THF solution of L^{NMe2} (1.0 g, 3.1 mmol). After the workup and purification, KL^{NMe2} remained as a white powder. Yield: 0.78 g (70%). ^{1}H NMR (360 MHz, benzene-d_6): δ 1.46 (s, 15H, $C(CH_3)_3$, $N(CH_3)_2$), 1.73 (s, 9H, $C(CH_3)_3$), 1.88 (s, 3H, NCH_3), 2.32 (s, 4H, NCH_2CH_2N), 3.57 (s, 2H, Ar−CH_2N), 7.08 (d, $^4J_{H-H}$ = 2.17 Hz, 1H, Ar−*H*), 7.48 (d, $^4J_{H-H}$ = 2.66 Hz, 1H, Ar−*H*). ^{13}C NMR (360 MHz, benzene-d_6): δ 30.8 ($C(CH_3)_3$), 32.8 ($C(CH_3)_3$), 34.3 ($C(CH_3)_3$), 36.1 ($C(CH_3)_3$), 43.9 (NCH_2CH_2N), 44.8 ($N(CH_3)_2$), 52.0 (NCH_2CH_2N), 57.7 (NCH_3), 63.3 (Ar−CH_2N), 123.3 (*Ar*), 123.4 (*Ar*), 124.7 (*Ar*), 130.1 (*Ar*), 136.6 (*Ar*), 167.4 (*Ar*−OK).

Anal. Calcd for $C_{20}H_{35}N_2OK$: C, 66.99; H, 9.84; N, 7.81. Found: C, 66.94; H, 9.81; N, 8.04%.

General Synthetic Procedures for Molybdenum Complexes. The respective ligand (1 equiv) was dissolved in 10 mL of toluene and slowly added to a solution of [$MoO_2Cl(\eta^2$-*t*-$Bu_2pz)$] (1 equiv) in 10 mL of toluene. The formation of the complex was immediately indicated by a change of color. After stirring the mixture for 15 min at room temperature, the mixture was filtered through a pad of Celite and the solvent removed in vacuo. The residue was washed twice with pentane, affording the pure compounds as yellow to orange solids. Crystals suitable for X-ray diffraction analysis were obtained from a concentrated benzene solution.

Synthesis of [$MoO_2Cl(L^{OMe})$] (1). The synthesis of complex **1** followed the general procedure described above. A solution of the ligand HL^{NO} (0.12 g, 0.37 mmol) in toluene was added to a suspension of [$MoO_2Cl(\eta^2$-*t*-$Bu_2pz)$] (0.13 g, 0.37 mmol) in toluene. After purification, complex **1** was obtained as a yellow solid. Yield: 0.14 g (79%). ^{1}H NMR (360 MHz, benzene-d_6): δ 1.33 (s, 9H, C(CH_3)$_3$), 1.56 (s, 9H, C(CH_3)$_3$), 1.76 (m, 1H, CH_2), 2.20 (m, 1H, CH_2), 2.44 (m, 1H, CH_2), 2.50 (s, 3H, NCH_3), 2.95 (d, $^2J_{H-H}$ = 14.1 Hz, 1H, Ar−CH_2N), 2.98 (m, 1H, CH_2), 3.48 (s, 3H, OCH_3), 4.01 (d, $^2J_{H-H}$ = 13.9 Hz, 1H, Ar−CH_2N), 6.80 (d, $^4J_{H-H}$ = 2.27 Hz, 1H, Ar−*H*), 7.51 (d, $^4J_{H-H}$ = 2.37 Hz, 1H, Ar−*H*). ^{13}C (360 MHz, benzene-d_6): δ 30.6 (C(*C*H_3)$_3$), 32.2 (C(*C*H_3)$_3$), 34.9 (*C*(CH$_3$)$_3$), 35.7 (*C*(CH$_3$)$_3$), 50.1 (N*C*H$_3$), 55.1 (N*C*H$_2$CH$_2$O), 63.5 (Ar−*C*H$_2$N), 63.8 (O*C*H$_3$), 69.0 (NCH$_2$-*C*H$_2$O), 123.8 (*Ar*), 124.6 (*Ar*), 124.7 (*Ar*), 138.2 (*Ar*), 144.2 (*Ar*), 158.4 (*Ar*−O). MS (EI) (70 eV) *m*/*z* (%): 470 (7) [M$^+$], 425 (36) [M$^+$ − CH$_3$OCH$_2$], 382 (81) [M$^+$ − CH$_3$O(CH$_2$)$_2$NCH$_3$], 219 (100) [$C_{15}H_{23}O^+$], 57 (7) [C(CH$_3$)$_3^+$]. Anal. Calcd for $C_{19}H_{32}NO_4MoCl$: C, 48.57%; H, 6.86%; N, 2.98%; Found: C, 48.76%; H, 6.88%; N, 2.97%.

Synthesis of [$MoO_2Cl(L^{SEt})$] (2). Complex **2** was prepared using a similar procedure to that of complex **1**. A solution of the ligand HL^{NS} (0.18 g, 0.54 mmol) in 10 mL of toluene was added to a suspension of [$MoO_2Cl(\eta^2$-*t*-$Bu_2pz)$] (0.19 g, 0.54 mmol) in 10 mL of toluene. Complex **2** was obtained as a red solid. Yield: 0.27 g (71%). ^{1}H NMR (360 MHz, benzene-d_6): δ 1.01 (t, $^3J_{H-H}$ = 7.40 Hz, 3H, SCH$_2$CH_3), 1.33 (s, 9H, C(CH_3)$_3$), 1.57 (s, 9H, C(CH_3)$_3$), 1.94 (m, 2H, CH_2), 2.12 (m, 2H, CH_2), 2.32 (m, 1H, CH_2), 2.47 (m, 1H, CH$_2$), 2.58 (s, 3H, NCH_3), 2.90 (d, $^2J_{H-H}$ = 12.7 Hz, 1H, Ar−CH_2N), 4.12 (d, $^2J_{H-H}$ = 13.0 Hz, 1H, Ar−CH_2N), 6.81 (d, $^4J_{H-H}$ = 2.16 Hz, 1H, Ar−*H*), 7.50 (d, $^4J_{H-H}$ = 2.06 Hz, 1H, Ar−*H*). ^{13}C NMR (360 MHz, benzene-d_6): δ 12.9 (SCH$_2$*C*H$_3$), 30.6 (S*C*H$_2$CH$_3$), 30.8 (C(*C*H$_3$)$_3$), 31.0 (N*C*H$_2$CH$_2$S) 32.1 (C(*C*H$_3$)$_3$), 34.9 (*C*(CH$_3$)$_3$), 35.7 (*C*(CH$_3$)$_3$), 50.6 (N*C*H$_3$), 56.7 (N*C*H$_2$CH$_2$S), 64.2 (Ar−*C*H$_2$N), 123.9 (*Ar*), 124.8 (2 × *Ar*), 138.8 (*Ar*), 144.5 (*Ar*), 158.9 (*Ar*−O). MS (EI) (70 eV) *m*/*z* (%): 500 (6) [M$^+$], 425 (43) [M$^+$ − CH$_3$CH$_2$SCH$_2$], 383 (100) [M$^+$ − CH$_3$CH$_2$S(CH$_2$)$_2$NCH$_3$)], 262 (23) [M$^+$ − CH$_3$CH$_2$-SCH$_2$MoO$_2$Cl], 219 (73) [$C_{15}H_{23}O^+$], 57 (50) [C(CH$_3$)$_3^+$]. Anal. Calcd for $C_{20}H_{34}NO_3SMoCl$: C, 48.07; H, 6.86; N, 2.80. Found: C, 47.80; H, 6.87; N, 3.07%.

Synthesis of [$MoO_2Cl(L^{NEt2})$] (3). A solution of the ligand HL^{NEt2} (0.27 g, 0.76 mmol) in 10 mL of toluene was slowly added to a suspension of [$MoO_2Cl(\eta^2$-*t*-$Bu_2pz)$] (0.26 g, 0.76 mmol) in 10 mL of toluene. The solution changed color to red immediately. After purification, complex **3** was obtained as an orange solid. Yield: 0.28 g (73%). ^{1}H NMR (360 MHz, benzene-d_6; isomer A and isomer B): δ 0.78 (t, $^3J_{H-H}$ = 7.1 Hz, 3H, NCH$_2$CH_3), 0.83 (t, $^3J_{H-H}$ = 7.0 Hz, 3H, NCH$_2$CH_3), 0.87 (t, $^3J_{H-H}$ = 6.9 Hz, 3H, NCH$_2$CH_3), 1.16 (t, $^3J_{H-H}$ = 7.1 Hz, 3H, NCH$_2$CH_3), 1.35 (s, 9H, C(CH_3)$_3$), 1.36 (s, 9H, C(CH_3)$_3$), 1.59 (s, 9H, C(CH_3)$_3$), 1.75 (s, 9H, C(CH_3)$_3$), 2.04 (m, 6H, NCH_2), 2.29 (m, 2H, NCH_2), 2.61 (s, 3H, NCH_3), 2.63 (m, 4H, NCH_2), 2.66 (s, 3H, NCH_3), 2.87 (d, $^2J_{H-H}$ = 14.2 Hz, 1H, Ar−CH_2N), 3.09 (m, 2H, NCH_2), 3.21 (d, $^2J_{H-H}$ = 14.2 Hz, 1H, Ar−CH_2N), 3.43 (m, 2H, NCH_2), 3.61 (d, $^2J_{H-H}$ = 14.1 Hz, 1H, Ar−CH_2N), 4.70 (d, $^2J_{H-H}$ = 14.6 Hz, 1H, Ar−CH_2N), 6.84 (d, $^4J_{H-H}$ = 2.39 Hz, 1H, Ar−*H*), 6.91 (d, $^4J_{H-H}$ = 2.39 Hz, 1H, Ar−*H*), 7.51 (d, $^4J_{H-H}$ = 2.34 Hz, 1H, Ar−*H*), 7.57 (d, $^4J_{H-H}$ = 2.38 Hz, 1H, Ar−*H*). ^{13}C NMR (360 MHz, benzene-d_6; isomer A and isomer B): δ 8.1 (N*C*H$_3$), 8.4 (N*C*H$_3$), 9.2 (N*C*H$_3$), 10.0 (N*C*H$_3$), 31.2 (C(*C*H$_3$)$_3$), 31.5 (C(*C*H$_3$)$_3$), 32.2 (C(*C*H$_3$)$_3$), 32.3 (C(*C*H$_3$)$_3$), 35.1 (*C*(CH$_3$)$_3$), 35.6 (*C*(CH$_3$)$_3$), 35.8 (*C*(CH$_3$)$_3$), 36.1 (*C*(CH$_3$)$_3$), 47.6 (N*C*H$_2$-CH$_3$), 47.7 (N*C*H$_2$CH$_3$), 48.6 (N*C*H$_3$), 49.0 (N*C*H$_2$CH$_3$), 50.3 (N*C*H$_3$), 50.6 (N*C*H$_2$CH$_3$), 53.1 (NCH$_2$*C*H$_2$N), 53.9 (NCH$_2$-*C*H$_2$N), 55.2 (N*C*H$_2$CH$_2$N), 55.4 (N*C*H$_2$CH$_2$N), 63.3 (Ar−*C*H$_2$N), 66.2 (Ar−*C*H$_2$N), 124.2 (*Ar*), 124.3 (*Ar*), 124.4 (*Ar*), 124.5 (*Ar*), 124.8 (*Ar*), 124.9 (*Ar*), 136.9 (*Ar*), 139.8 (*Ar*), 143.1 (*Ar*), 144.2 (*Ar*), 157.9 (*Ar*−O), 162.3 (*Ar*−O). MS (EI) (70 eV) *m*/*z* (%): 511 (1) [M$^+$], 476 (2) [M$^+$ − Cl], 382 (1) [Mo$^+$ − (CH$_3$-CH$_2$)$_2$N(CH$_2$)$_2$NCH$_3$], 348 (2) [M$^+$ − MoO$_2$Cl], 262 (4) [M$^+$ − (CH$_3$CH$_2$)$_2$NCH$_2$MoO$_2$Cl], 219 (10) [$C_{15}H_{23}O^+$], 86 (100) [(CH$_3$CH$_2$)$_2$NCH$_2^+$], 57 (10) [C(CH$_3$)$_3^+$]. Anal. Calcd for $C_{22}H_{39}N_2O_3MoCl$: C, 51.74; H, 7.70; N, 5.48. Found: C, 51.39; H, 7.74; N, 5.31%.

Synthesis of [$MoO_2Cl(L^{NMe2})$] (4). The synthesis of complex **4** followed the procedure described above. To a suspension of [$MoO_2Cl(\eta^2$-*t*-$Bu_2pz)$] (0.15 g, 0.45 mmol) in 10 mL of toluene was added a solution of the ligand HL^{NMe2} (0.14 g, 0.45 mmol) in 10 mL of toluene, affording complex **4** as a red solid. Yield: 0.15 g (67%). ^{1}H NMR (isomer A; 360 MHz, benzene-d_6): δ 1.35 (s, 3H, NCH_3), 1.37 (s, 9H, C(CH_3)$_3$), 1.67 (s, 3H, NCH_3), 1.72 (s, 9H, C(CH_3)$_3$), 2.38 (s, 3H, NCH_3), 2.68 (s, 4H, NCH_2CH_2N), 2.89 (d, $^2J_{H-H}$ = 14.09 Hz, 1H, Ar−CH_2N), 4.69 (d, $^2J_{H-H}$ = 13.83 Hz, 1H, Ar−CH_2N), 6.85 (d, $^4J_{H-H}$ = 2.02 Hz, 1H, Ar−*H*), 7.56 (d, $^4J_{H-H}$ = 2.10 Hz, 1H, Ar−*H*). ^{13}C NMR (360 MHz, benzene-d_6): δ 30.8 (C(*C*H$_3$)$_3$), 31.7 (C(*C*H$_3$)$_3$), 34.3 (*C*(CH$_3$)$_3$), 35.5 (*C*(CH$_3$)$_3$), 48.0 (N*C*H$_3$), 48.1 (N*C*H$_3$), 52.1 (N*C*H$_3$), 55.7 (NCH$_2$*C*H$_2$N), 58.8 (N*C*H$_2$CH$_2$N), 65.3 (Ar−*C*H$_2$N), 123.9 (*Ar*), 124.5 (*Ar*), 124.7 (*Ar*), 139.1 (*Ar*), 142.5 (*Ar*), 157.1 (*Ar*−O). ^{1}H NMR (isomer B; 360 MHz, benzene-d_6): δ 1.25 (s, 3H, NCH_3), 1.35 (s, 9H, C(CH_3)$_3$), 1.53 (s, 12H, C(CH_3)$_3$, NCH_3), 2.21 (s, 3H, NCH_3), 2.58 (s, 4H, NCH_2CH_2N), 3.17 (d, $^2J_{H-H}$ = 14.55 Hz, 1H, Ar−CH_2N), 4.12 (d, $^2J_{H-H}$ = 14.10 Hz, 1H, Ar−CH_2N), 6.88 (d, $^4J_{H-H}$ = 2.15 Hz, 1H, Ar−*H*), 7.50 (d, $^4J_{H-H}$ = 2.18 Hz, 1H, Ar−*H*). ^{13}C NMR (360 MHz, benzene-d_6): δ 30.6 (C(*C*H$_3$)$_3$), 31.6 (C(*C*H$_3$)$_3$), 34.3 (*C*(CH$_3$)$_3$), 35.1 (*C*(CH$_3$)$_3$), 49.4 (N*C*H$_3$), 50.3 (N*C*H$_3$), 52.1 (N*C*H$_3$), 54.2 (NCH$_2$*C*H$_2$N), 56.4 (N*C*H$_2$CH$_2$N), 63.8 (Ar−*C*H$_2$N), 122.9 (*Ar*), 123.8 (*Ar*), 123.9 (*Ar*), 137.0 (*Ar*), 143.6 (*Ar*), 159.1 (*Ar*−O). MS (EI) (70 eV) *m*/*z* (%): 483 (1) [M$^+$], 448 (5) [M$^+$ − Cl], 425 (1) [M$^+$ − (CH$_3$)$_2$NCH$_2$], 382 (4) [M$^+$ − (CH$_3$)$_2$N(CH$_2$)$_2$NCH$_3$], 320 (1) [M$^+$ − MoO$_2$Cl], 262 (4) [M$^+$ − (CH$_3$)$_2$NCH$_2$MoO$_2$Cl], 219 (12) [$C_{15}H_{23}O^+$], 58 (100) [(CH$_3$)$_2$NCH$_2^+$], 57(12) [C(CH$_3$)$_3^+$]. Anal. Calcd for $C_{20}H_{35}$-N_2O_3MoCl: C, 50.74; H, 7.46; N, 6.88. Found: C, 50.71; H, 7.45; N, 6.49%.

Preparation of Molybdenum(VI)dioxo Complexes via Deprotonation of the Ligand with Et$_3$N. A solution of the relevant ligand (0.33 mmol) in toluene was slowly added to a solution of 65 mg of [MoO_2Cl_2] (0.33 mmol) in toluene at room temperature. The mixture was stirred for 5 min, and then 150 μL of Et$_3$N was added. The formation of the complex was indicated by the change of color. After the mixture was stirred for at most 2 h, the colored solution was filtered through a pad of Celite and the solvent removed in a vacuum to afford a waxy product. The residue was washed several times with pentane to give a solid product [yield: complex **1**, 117 mg (71%); complex **2**, 69 mg (42%); complex **4**, 64 mg (41%)]. The synthesis of complex **3** has not proved satisfactory.

Preparation of Molybdenum(VI)dioxo Complexes via the Potassium Salt of the Ligand. The potassium salt of the ligand (0.25 mmol) was dissolved in THF and slowly added to a solution of 50 mg of [MoO_2Cl_2] (0.25 mmol) in THF. The formation of the complex was immediately indicated by a change of color. The mixture was stirred overnight and then filtered through a pad of

Celite. The colored solution was concentrated under a vacuum, and the obtained residue was washed several times with pentane to give a solid product. In order to remove the remaining salt, the product was dissolved in toluene and filtered through a pad of Celite. The solution was again concentrated under a vacuum to obtain the pure compound as a solid product [yield: complex **1**, 73 mg (62%); complex **2**, 73 mg (58%); complex **3**, 70 mg (54%); and complex **4**, 69 mg (57%)].

Computational Details. All calculations were performed using the Gaussian 03 software package on the Phoenix Linux Cluster of the Vienna University of Technology.[53] In all model complexes, the *tert*-butyl group in the para position of the phenol has been replaced by hydrogen to reduce calculation time. The geometries and energies of the model complexes and the transition states were optimized at the B3LYP level[54−56] with the Stuttgart/Dresden ECP (SDD) basis set[57−59] to describe the electrons of the molybdenum atom. For all other atoms, the 6-31 g** basis set was employed.[60−66] A vibrational analysis was performed to confirm that the structures of the model compounds have no imaginary frequency. All geometries were optimized without symmetry constraints.

Proton chemical shifts were calculated at the B3LYP level of theory for the optimized structures of **C1**−**C5** using the GIAO method in Gaussian 03 with the same basis sets as above. Chemical shifts are given with respect to $Si(Me_3)_4$ (TMS) at the same computational level.

X-Ray Structure Determination. For X-ray structure analyses for compounds HL^{OMe}, KL^{NMe2}, **2**, and **3**, the crystals were mounted onto the tips of glass fibers. Data collection for compounds HL^{OMe}, **2**, and **3** were performed with a Bruker-AXS SMART APEX CCD diffractometer using graphite-monochromated Mo Kα radiation (0.71073 Å). Data of compound KL^{NMe2} were collected on a Stoe four-cycle diffractometer using graphite-monochromatized Mo Kα radiation (0.71069 Å). The data for all compounds were reduced to F_o^2, and absorption effects were corrected either empirically for KL^{NMe2} or with SAINT[67] and SADABS[68] for all other compounds, respectively. The structures were solved by direct methods[69] and refined by the full-matrix least-squares method.[70] If not noted otherwise, all non-hydrogen atoms were refined with anisotropic displacement parameters. All hydrogen atoms were located in calculated positions to correspond to standard bond lengths and angles. All diagrams were drawn with 30% probability thermal ellipsoids, and all hydrogen atoms have been omitted for clarity. In compound KL^{NME2}, one dimethylamino group (N64) is disordered over two orientations [site occupation factors of 0.863(3) and 0.137(3)]. By inclusion of the less occupied atomic positions (isotropic refinement without any constraints of the C atoms, the H atoms included at calculated positions with their isotropic displacement parameters fixed to 1.2 times U_{eq} of the C atom they are bonded to), the R factor R1 dropped from 0.0506 to 0.0439. The pendant arm in complex **2** is split over two positions with occupancies that refined to 68% and 32%. Attempts to include the pivot atom C15 in the splitting components did not lead to an overall improvement of the R factor, so it was left with a high thermal parameter.

Crystallographic data (excluding structure factors) for the structures of compounds HL^{OMe}, KL^{NMe2}, **2**, and **3** reported in this paper have been deposited with the Cambridge Crystallographic Data Center as supplementary publication numbers CCDC-736559 (HL^{OMe}), 737219 (KL^{NMe2}), 736558 (**2**), and 736557 (**3**). Copies of the data can be obtained free of charge on application to The Director, CCDC, 12 Union Road, Cambridge CB2 1EZ, U. K. [fax: (international) +44−1223/336-033; e-mail: deposit@ccdc.cam.ac.uk].

Acknowledgment. We thank Dr. Anna Sachse for the help in the preparation of compound **2**. Generous support for this work by a grant from Fonds zur Förderung der Wissenschaftlichen Forschung (FWF) (Projektnr. P19309-N19) is gratefully acknowledged.

Supporting Information Available: Optimized geometries and relative free energies (in kcal/mol) with facial and meridional geometries of the tridentate ligands L^{OMe} and L^{SMe}. Profile of the B3LYP potential energy surfaces (free energies in kcal/mol) for the conversion of $\mathbf{A^1(S)}$ to the mer isomer **C4** with internal NMe moiety adopting an R or S configuration. Crystallographic data in CIF format for HL^{OMe}, KL^{NMe2}, **2**, and **3**. This material is available free of charge via the Internet at http://pubs.acs.org.

(54) Becke, A. D. *J. Chem. Phys.* **1993**, *98*, 5648–5652.
(55) Miehlich, B.; Savin, A.; Stoll, H.; Preuss, H. *Chem. Phys. Lett.* **1989**, *157*, 200–206.
(56) Lee, C.; Yang, W.; Parr, G. *Phys. Rev. B* **1988**, *37*, 785–789.
(57) Haeusermann, U.; Dolg, M.; Stoll, H.; Preuss, H. *Mol. Phys.* **1993**, *78*, 1211–1224.
(58) Kuechle, W.; Dolg, M.; Stoll, H.; Preuss, H. *J. Chem. Phys.* **1994**, *100*, 7535–7542.
(59) Leininger, T.; Nicklass, A.; Stoll, H.; Dolg, M.; Schwerdtfeger, P. *J. Chem. Phys.* **1996**, *105*, 1052–1059.
(60) McLean, A. D.; Chandler, G. S. *J. Chem. Phys.* **1980**, *72*, 5639–5648.
(61) Krishnan, R.; Binkley, J. S.; Seeger, R.; Pople, J. A. *J. Chem. Phys.* **1980**, *72*, 650–654.
(62) Wachters, A. J. H. *J. Chem. Phys.* **1970**, *52*, 1033–1036.
(63) Hay, P. J. *J. Chem. Phys.* **1977**, *66*, 4377–4384.
(64) Raghavachari, K.; Trucks, G. W. *J. Chem. Phys.* **1989**, *91*, 1062–1065.
(65) Binning, R. C.; Curtiss, L. A. *J. Chem. Phys.* **1995**, *103*, 6104–6113.
(66) McGrath, M. P.; Radom, L. *J. Chem. Phys.* **1991**, *94*, 511–516.
(67) *SAINTPLUS: Software Reference Manual*, version 6. 4; Bruker AXS: Madison, WI, 1997.
(68) Blessing, R. H. *Acta Crystallogr., Sect. A* **1995**, *51*, 33−38. *SADABS*, version 2.1; Bruker-AXS: Madison, WI, 1998
(69) Sheldrick, G. M. *SHELXS-97*; University of Göttingen: Göttingen, Germany, 1997.
(70) Sheldrick, G. M. *SHELXL-97*; University of Göttingen: Göttingen, Germany, 1997.